Journal of Peptide Science
J. Peptide Sci. **10**: 678–690 (2004)
Published online 10 June 2004 in Wiley InterScience (www.interscience.wiley.com). DOI: 10.1002/psc.576

JOURNAL OF PEPTIDE SCIENCE

Solution Conformational Study of Nociceptin and its 1–13 and 1–11 Fragments Using Circular Dichroism and Two-dimensional NMR in Conjunction with Theoretical Conformational Analysis

LIDIA KLAUDEL,[a] ANNA ŁĘGOWSKA,[a] KRZYSZTOF BRZOZOWSKI,[a] JERZY SILBERRING,[b] JACEK WÓJCIK[c] and KRZYSZTOF ROLKA[a]*

[a] Faculty of Chemistry, University of Gdańsk, Sobieskiego 18, 80-952 Gdańsk, Poland
[b] Faculty of Chemistry and Regional Laboratory, Jagiellonian University, Ingardena 3, 30-060 Kraków, Poland
[c] Laboratory of Biological NMR, Institute of Biochemistry and Biophysics, Polish Academy of Sciences, Pawińskiego 5a, 02-106 Warszawa, Poland

Received 19 January 2004
Revised 11 July 2004
Accepted 17 July 2004

Abstract: Conformational studies of nociceptin (NC-NH_2), its fully active fragment, NC(1–13)-NH_2, and two significantly less potent fragments, NC(1–13)-OH and NC(1–11)-OH, were conducted in water and TFE solutions by the employment of circular dichroism, and in DMSO-d_6 by 2D NMR spectroscopy in conjunction with theoretical conformational analysis. The conformations of all the peptides studied were calculated taking two approaches. The first assumes multiconformational equilibrium of the peptide studied, which is characterized by a set of conformations (and their statistical weight values) obtained from a global conformational analysis using three methods: the electrostatically driven Monte-Carlo (EDMC) with the ECEPP/3 force field, the simulated annealing (SA) protocols in the AMBER and CHARMM force fields. The second approach incorporates the interproton distance and dihedral angle constraints into the starting conformation. Calculations were performed using the distance geometry and SA protocol in the CHARMM force field implemented in the X-PLOR program. The CD experiments indicated that for the active peptides, hydrophobic solvents induced a significantly higher (compared with those remaining) content order, probably a helical structure. Unfortunately, as a result of the conformational flexibility of the peptides, the analysis of conformations obtained with both approaches and different force fields did not allow the selection of any structural elements of the NC peptides that might be connected with their bioactivity. The only common element found in most conformations of the active peptides was a helical character of fragment 8–13, which allowed the side chains of basic amino acid residues to be exposed to the outside of the molecule and probably to interact with the ORL1 receptor. Copyright © 2004 European Peptide Society and John Wiley & Sons, Ltd.

Keywords: nociceptin; fragments; conformational studies; CD spectroscopy; NMR spectroscopy

* Correspondence to: Dr Krzysztof Rolka, University of Gdańsk, Sobieskiego 18, 80-952 Gdańsk, Poland;
e-mail: krzys@chemik.chem.univ.gda.pl
Contract/grant sponsor: University of Gdańsk; Contract/grant numbers: BW-8000-5-0182-1; DS/8290-4-0129-3.
Contract/grant sponsor: Polish Committee for Scientific Research; Contract/grant number: KBN 3P04B02024.
Contract/grant sponsor: Adam Krzyzanowski Foundation.

INTRODUCTION

In 1995, two groups independently isolated a 17-amino acid peptide (Phe-Gly-Gly-Phe-Thr-Gly-Ala-Arg-Lys-Ser-Ala-Arg-Lys-Leu-Ala-Asn-Gln) from two brain regions, the amygdala and the hypothalamus, areas known to regulate reactions to stressful events such as pain and fear [1,2]. Based on the observation that this peptide binds to a separate orphan receptor (ORL1, OP4) and inhibits the antinociceptive effects of morphine and opioid peptides, it was named orphanin FQ or nociceptin (NC). As shown recently [3], a proteinase present in the spinal cord released two major metabolites: NC(1–11) and NC(1–6). Their action after i.c.v. injections in rats exhibited a biphasic effect. Unlike NC, antinociception for up to 10 min was observed, followed by hyperalgesia [3]. The NMR conformational study of NC has shown [4] that in water and other solvents, the peptide displayed little tendency to form an ordered structure. On the other hand, as reported by the same group [5], the solution structure of dynorphin A, an opioid peptide with high sequential homology to NC, is significantly more ordered in the middle part of the molecule. In a cryoprotective solvent mixture, a large loop in fragment 7–13 was found with Pro10 at its apex [5]. The position of the side chains of the basic amino acid residues Arg7, Lys11 and Lys13, crucial for the activity, allows interaction with the acidic amino acid residues of the e2 loop of the κ opioid receptor [5]. The comparison of solution structures of both peptides led the authors to the conclusion that the presence of the Pro10 residue in the dynorphin A sequence significantly rigidified the conformation of its *C*-terminal fragment. Bearing this in mind, the Italian group carried out very recently [6] a conformational analysis of NC(1–13)-NH_2 — a peptide as active in pharmacological tests as the parent compound [7], and its three analogues with the Pro residue in position 5, 6 and 7, respectively. Of these, only the analogue with the Pro residue in position 6 displayed some activity (two orders of magnitude lower than that of NC) in the MVD test [6]. A comparison of the NMR data and the pharmacological profiles of the peptides led to the conclusion that the activity of nociceptin might be associated with the presence of the β-turn centred on Gly^6-Ala^7 [6]. Although the Pro residue introduced into the NC peptides rigidified their structures, the number of NOE effects observed for NC and other NC peptides did not allow a reliable conformational analysis with a sufficient number of conformational constraints.

In order to obtain more details about the solution conformation of NC, conformational analysis was performed of the NC peptides NC-NH_2, NC(1–13)-NH_2, NC(1–13)-OH and NC(1–11)-OH. The sequences selected for the analysis were based on reports [7,8] postulating that NC and fragment 1–13 with an amide moiety at the *C*-terminus retained the full agonistic activity of the parent compound, whereas fragment 1–13 with the *C*-terminal carboxyl group was considerably less potent and lost the receptor activity. Shorter fragments (including 1–11) did not show the NC activity. It was assumed that a comparison of the solution structures obtained for all four peptides displaying different pharmacological profiles might identify structural elements responsible for the NC activity. Two methods were applied in this study. The first was CD spectroscopy, which in a short time provided information on the global peptide conformation. The investigations were conducted in water and TFE solutions. TFE is a solvent frequently used to study solution conformations of biologically active peptides. The second method was NMR spectroscopy in conjunction with theoretical calculations. In this experiment, DMSO-d_6 was used as the solvent. In view of the high conformational flexibility of the peptides, the analysis was carried out with two different approaches, calculating the peptide conformations by the use of three different force fields.

MATERIALS AND METHODS

Peptide Synthesis

All peptides were synthesized by the solid-phase method using the Fmoc chemistry. TentaGel S RAM (substitution of the Fmoc groups 0.22 meq/g) and TentaGel S AC (substitution of the Fmoc groups 0.20 meq/g) (RAPP Polymere, Germany) were used as a support. The peptides were synthesized by the same procedure as described in our previous paper [9].

CD Experiment

The peptide concentrations were 0.29 mM for NC-NH_2, 0.39 mM for NC(1–13)-NH_2 and NC(1–13)-OH, 0.48 mM for NC(1–11)-OH in water and TFE solutions. The CD spectra were obtained at room temperature on a Jasco J-20 spectropolarimeter, operating in the 260–190 nm range, automated

and equipped with a program prepared by Medson (Poland). 1 mm quartz cells were used. The results were plotted as the mean residue ellipticity $[\Theta]_r$ [degree $\times$ cm^2 $\times$ dmol^{-1}].

NMR Experiment

The sample concentrations were 5.5 mM for NC-NH_2, 7.2 mM for NC(1–13)-NH_2 and NC(1–13)-OH, 9.1 mM for NC(1–11)-OH in 0.7 ml DMSO-d_6. The ^{1}H-NMR experiments of NC-NH_2 and NC(1–13)-OH were performed on a Unity500plus (Varian) operating at 500.6 MHz resonance frequency. A Varian mercury spectrometer operating at 400 MHz resonance frequency was used for NC(1–13)-NH_2 and NC(1–11)-OH. All 2D ^{1}H-NMR spectra were recorded at 303 K. One-dimensional spectra, which were used to calculate the temperature coefficients of the chemical shifts for the amide proton resonances ($\Delta\delta/\Delta T$), were recorded in the temperature range 295–333 K. In the case of NC-NH_2 and NC(1–11)-OH, a mixing time of 90 ms was used for the TOCSY [10] and DQF-COSY [11,12] spectra, 300 ms for the NOESY [13,14] and 200 ms for the ROESY [15,16] spectra (only for NC-NH_2). For fragments 1–13, a mixing time of 80 ms was used for the NOESY spectra, 90 ms for the DQF-COSY, 50 ms for the TOCSY spectra and 200 ms for the ROESY spectra (only for NC(1–13)-OH). Proton chemical shifts were assigned using the 1D and 2D ^{1}H-NMR spectra. The data were processed using the XEASY program [17] on a SUN Ultrasparc workstation.

The $^3J_{NH\text{-}H\alpha}$ coupling constants were extracted from 1D ^{1}H-NMR spectra at 303K after resolution enhancement recorded at 500 MHz for NC-NH_2 and NC(1–13)-OH, and 400 MHz for NC(1–13)-NH_2 and NC(1–11)-OH. These data were processed using the MestRe-C 2.3 program [18].

The values of $\Delta\delta/\Delta T$ were calculated from the 1D ^{1}H-NMR spectra recorded at 295 K, 303 K, 308 K, 313 K and 318 K for NC-NH_2 and NC(1–11)-OH, whereas for fragments 1–13 the 1D spectra were recorded at 295 K, 303 K, 313 K, 323 K and 333 K. The NOE cross-peaks of the peptides studied picked up on the NOESY spectra. The inter-proton distances and the torsion angles were generated using the CALIBA and HABAS algorithms, respectively, of the DIANA package [19].

Conformational Calculations

Three-dimensional solution structures of the peptides were determined taking two approaches:

1. A global conformational search of all four peptides was performed using the electrostatically driven Monte-Carlo (EDMC) method with the ECEPP/3 force field and simulated annealing protocol (SA), implemented in AMBER and CHARMM force fields. The NOE effects and the $^3J_{NH\text{-}H\alpha}$ coupling constants were computed for the conformations obtained, and then statistical weights of these conformations were calculated by fitting the theoretical NOE effects and $^3J_{NH\text{-}H\alpha}$ coupling constants values to the experimental NMR data.
2. The distance geometry and SA protocols implemented in the X-PLOR program were used. The 3D structure of each peptide was computed using interproton distances calculated from the NOE intensities and torsion angles calculated from vicinal coupling constants as constraints.

Force Fields

A search of the conformational space was first conducted by the electrostatically driven Monte Carlo (EDMC) method [20]. Conformational energy was evaluated using the ECEPP/3 (empirical conformational energy program for peptides) force field [21] that assumes rigid valence geometry. The total conformational energy (E_{tot}) was a sum of the electrostatic energy (E_{es}), nonbonded energy (E_{nb}) and torsional energy (E_{tor}). The force field included solvation free energy (E_{solv}), which was calculated using the surface-solvation model parameterized to describe the energy of solvation in DMSO [22].

Conformational space was also searched for using the simulated annealing algorithm with the AMBER 4.1 [23] and 5.0 [24] and CHARMM [25] (from X-PLOR 3.1 [26]) force fields not including the solvent. The total conformational energy (E_{tot}) in the AMBER calculation was a sum of the electrostatic energy (E_{es}), bonded energy (E_b), hydrogen bond energy (E_{hb}), valence angles energy (E_{ang}) and torsion angles energy (E_{dh}). In the CHARMM force field, electrostatic interactions and the energy of hydrogen bonds were not directly included, and van der Waals interactions were described with a simplified potential function. According to the NMR data, the geometry of the peptide bonds was fixed to *trans*. The chirality of all αC (except for the Gly residues) was fixed to L.

EDMC calculations. The software used was the ECEPPAK global conformational analysis package [27]. Finally, 3000 energy-minimized conformations were obtained for each peptide studied. The

ensembles of the final conformations were clustered (using the minimum variance algorithm [28]). The root mean square deviation (RMSD) between the heavy atoms at an optimum superposition was taken as a measure of the distance between conformations, and a cut-off value of 3.0 Å was used to separate the families for each of the peptides. In the case of NC-NH_2, 1334 families were obtained, for NC(1–13)-NH_2 — 1025, for NC(1–13)-OH — 1087 and for NC(1–11)-OH — 578 families were selected.

Simulated annealing algorithm. The starting conformation was set to the helical form for NC-NH_2, the extended form for other peptides in the AMBER force field and a random structure for all the peptides studied in the CHARMM force field. In the AMBER force field, the SA algorithm lasted 15 ps and consisted of three steps: the molecule was fast heated at 1200 K for 1 ps, annealed at this temperature for 2 ps and slowly cooled for the last 12 ps. The ramping method (exponential ramping) was applied for the annealing (temperature vs time). In the case of the CHARMM force field, the cycle of the SA algorithm consisted of the following steps: the molecule was heated to 1000 K, annealed at this temperature for 50 ps (25 000 steps) and slowly cooled to 100 K for the last 30 ps (15 000 iterations). Additionally, the Powell minimization was performed during the last 200 iterations. Finally, 1000 energy-minimized conformations in each of these two force fields were obtained for each peptide.

Calculations of statistical weights of the conformations obtained. The statistical weights of all conformations (obtained in the AMBER and CHARMM force fields) and of the lowest-energy conformations from each family (obtained in the ECEPP/3 force field) were calculated by fitting the theoretical NOE spectra and $^3J_{NH\text{-}H\alpha}$ coupling constants to the experimental values, using the ANALYZE algorithm [29]. The intensities of NOE effects were computed by solving the Bloch differential equations system [30] applying the MORASS program [31, 32]. The $^3J_{NH\text{-}H\alpha}$ coupling constants were calculated from the empirical Bystrov–Karplus relationship [33].

Distance geometry. The structures of each peptide were created using the distance geometry and simulated annealing calculations applying the X-PLOR program [26]. Initial structures were generated by metric matrix distance geometry embedding using all atoms which were subjected to restrained simulated annealing followed by simulated annealing refinement. The molecule was heated and annealed at 2000 K for 3 ps (1000 steps) next cooled to 100 K for 5 ps (1000 steps) and in the last 200 steps the energy was minimized with the Powell algorithm

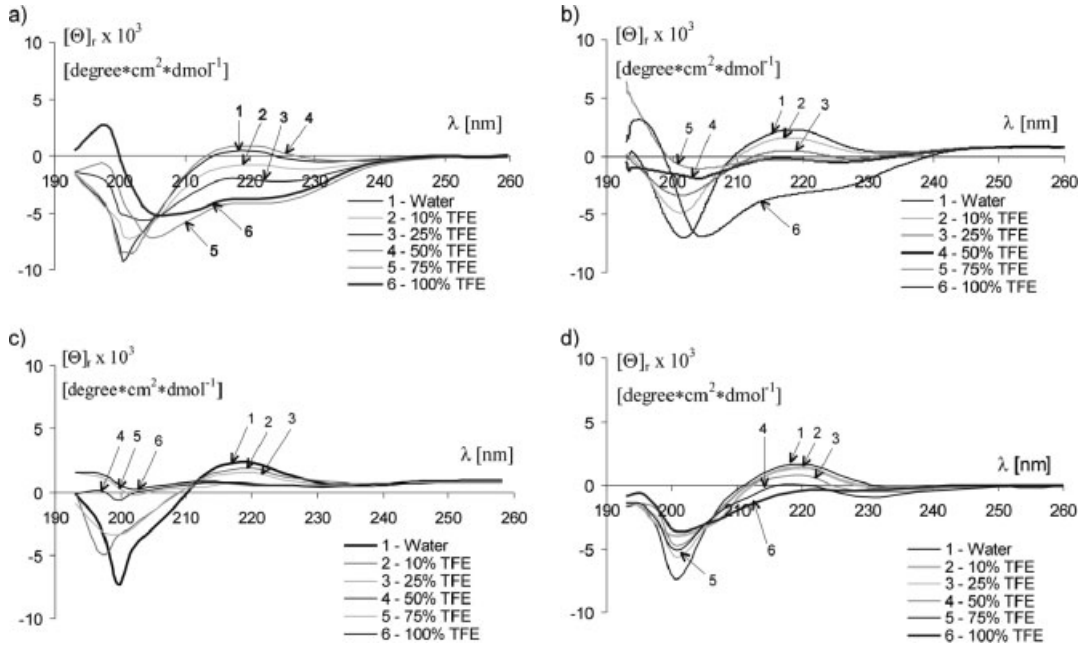

Figure 1 CD spectra in water and TFE solutions of the following peptides: (a) NC-NH_2 (0.29 mM); (b) NC(1–13)-NH_2 (0.39 mM); (c) NC(1–13)-OH (0.39 mM); (d) NC(1–11)-OH (0.48 mM).

[34]. During the refinement, the molecule was slowly cooled from 1000 to 100 K for 5 ps (2000 steps). The refinement procedure was performed twice. It resulted in 40 low-energy conformations.

RESULTS AND DISCUSSION

The CD spectra of NC-NH_2 and its fragments 1–13 and 1–11 are shown in Figure 1. In the case of two active peptides (NC-NH_2 and NC(1–13)-NH_2), the increased content of TFE developed a negative ellipticity in the region 200–240 nm of their CD spectra. Those recorded in pure TFE displayed two minima at 205 nm and around 225 nm and also a maximum at 195–198 nm. This might indicate that in this solvent a partial helical structure was formed. It should be noted that CD spectra recorded for model peptides displaying a strong negative ellipticity in the region 200–240 nm formed some β-turns [35, 36]. Considering the conformational flexibility of the peptides studied, equilibrium between different elements of the secondary structure in their solution structures cannot be excluded. TFE had a significantly weaker impact on the shapes of the CD spectra recorded for the remaining two inactive fragments, NC(1–13)-OH and NC(1–11)-OH. Nevertheless, negative ellipticity in the region 210–230 nm developed, suggesting that under these conditions some fraction of an ordered structure might be present. The results obtained indicate that in the hydrophobic environment that mimics biological membranes, NC-NH_2 and NC(1–13)-NH_2 adopted conformations with a detectable share of an ordered, probably helical, structure. The tendency to form any ordered structure was significantly less pronounced for inactive 1–13 and 1–11 fragments

Table 1 The Chemical Shifts (ppm) and Temperature Coefficients of NH Protons of NC-NH_2 in DMSO-d_6 at 30 °C

Residue	Chemical shifts (ppm)						$\Delta\delta/\Delta T \times 10^{-3}$
	H_N	α	β	γ	δ	Other	
Phe[1]	8.12	4.08	3.10			2,6H: 7.26	−3.12
			2.93			3,4,5: nr	
Gly[2]	8.75	3.80					−2.92
		3.74					
Gly[3]	8.12	3.74					−3.12
		3.66					
Phe[4]	8.12	4.62	3.06			2,6H: 7.26	−3.12
			2.79			3,4,5: nr	
Thr[5]	8.08	4.18	4.01	1.04		OH: 5.06	—
Gly[6]	8.02	3.74					−4.76
Ala[7]	7.99	4.18	1.22				−3.45
Arg[8]	7.75	4.08	1.91	1.74	2.04	εNH_2: 7.24, 7.17, 6.76	−2.61
Lys[9]	7.87	4.21	1.65	1.29	1.52	εCH_2 – 2.74; εNH_2 – 7.70	−3.82
Ser[10]	7.94	4.29	3.59				−3.96
			3.54				
Ala[11]	8.15	4.25	1.21				—
Arg[12]	7.75	4.08	1.92	1.77	2.05	εNH_2: 7.32, 7.08	−2.61
Lys[13]	8.09	4.21	1.69	1.47	1.57	εCH_2 – 3.06; εNH_2 – 7.63	—
Leu[14]	7.95	4.25	1.59	1.47	0.86		−3.84
					0.83		
Ala[15]	7.89	4.24	1.20				−1.79
Asn[16]	8.04	4.45	2.55			δ: 7.43, 6.93	−2.59
			2.46				
Gln[17]	8.01	4.20	1.66	1.48		no	−2.62
C-NH_2	no						

no, not observed; nr, not resolved.

with a *C*-terminal carboxyl group. Based on a good correlation between the pharmacological profiles of the peptides studied and their conformational behaviour it is postulated that although the NC peptides show a high degree of conformational freedom, in order to interact with the ORL1 receptor they should display a tendency to adopt an ordered, probably a helical structure.

The assignment of the proton chemical shifts was done using ^{1}H-NMR 2D spectra. These data and the temperature coefficients of the NH protons of the peptides are summarized in Tables 1–4. Figure 2 presents the NOE patterns and values of the $^3J_{NH\text{-}H\alpha}$ coupling constants. The analysis of these results indicates that none of the NOE patterns supported the presence of a canonical secondary structure. On the other hand, the values of $\Delta\delta/\Delta T$ lower than −3.5 ppm/K suggest that these amide protons might be involved in the formation of hydrogen bonds. They may stabilize the β-turns present in solution structures of all peptides, although their positions cannot be identified. This suggests that the solution structures of all the peptides studied are rather flexible under the experimental conditions used. Our results are consistent with those reported for the NC peptides in the literature [4, 6]. Nevertheless, the appearance of NH_i-NH_{i+1} and long-distance cross-peaks in the NOESY spectra of two active peptides suggest that their solution structures are defined better than those of the remaining inactive peptides.

For each peptide studied, one set of proton resonances was observed. The lack of a sequential signal $H\alpha(i) - H\alpha(i+1)$ in the NOESY spectra of all these peptides and the exchange cross-peaks in the ROESY spectra of NC-NH_2 and NC(1–13)-OH indicate that all the peptide bonds have *trans* geometry.

The NMR data indicate a high degree of conformational flexibility of the NC peptides. Therefore it was decided to carry out conformational calculations of their solution structures by two different approaches: using conformational constraints (interproton distances and torsion angles extracted from the NMR data) and a method that allows the selection of such conformations after a global conformational analysis, which satisfy the experimental NMR data. The conformational equilibrium of the

Table 2 The Chemical Shifts (ppm) and Temperature Coefficients of NH Protons of NC(1–13)-NH_2 in DMSO-d_6 at 30 °C

Residue	Chemical shifts (ppm)						$\Delta\delta/\Delta T \times 10^{-3}$
	H_N	α	β	γ	δ	Other	
Phe[1]	7.23	3.46	3.00			2,6: 7.16; 3,5: 7.35 4: nr	0.52
Gly[2]	8.60	3.88 3.60					−0.56
Gly[3]	8.19	3.75 3.65					−1.83
Phe[4]	8.32	4.52	3.12 2.92				−1.73
Thr[5]	8.55	4.20	4.05	1.06			−2.26
Gly[6]	8.32	3.72 3.65					−1.73
Ala[7]	8.10	4.12	1.24				—
Arg[8]	8.40	4.20	1.77	1.48	3.06	εNH_2: 7.61	−0.16
Lys[9]	8.08	4.11	1.64	1.35	1.54	εCH_2: 2.71	−3.91
Ser[10]	8.08	4.30	3.69 3.57				−3.91
Ala[11]	8.47	4.13	1.28				−2.61
Arg[12]	8.16	4.08	1.70	1.52	3.03	εNH_2: nr	−3.31
Lys[13]	7.69	4.06	1.64	1.30	1.49	εCH_2: 2.69	−1.49
C-NH_2	7.03						—

no, not observed; nr, not resolved.

Table 3 The Chemical Shifts (ppm) and Temperature Coefficients of NH Protons of NC(1–13)-OH in DMSO-d_6 at 30 °C

Residue	Chemical shifts (ppm)						$\Delta\delta/\Delta T \times 10^{-3}$
	H_N	α	β	γ	δ	Other	
Phe[1]	no	4.06	3.11			2,6H: 7.28	—
			2.92			3,4,5: nr	
Gly[2]	8.80	3.80					−6.92
		3.72					
Gly[3]	8.30	3.74					−3.45
		3.70					
Phe[4]	8.09	4.50	3.11			2,6H: 7.30;	−2.55
			2.88			3,4,5: nr	
Thr[5]	8.39	4.23	4.04	1.07		OH: no	−3.96
Gly[6]	8.41	3.83					−2.05
		3.60					
Ala[7]	8.15	4.13	1.23				−2.96
Arg[8]	8.17	4.21	1.71	1.48	3.06	εNH_2: 7.67	0.45
Lys[9]	7.94	4.12	1.70	1.34	1.61	εCH_2: 2.75	−4.26
					1.53		
Ser[10]	7.92	4.30	3.65				−4.26
			3.57				
Ala[11]	7.97	4.24	1.25				−2.78
Arg[12]	8.18	4.23	1.71	1.47	1.75	εNH_2: 8.03	0.45
Lys[13]	7.97	4.17	1.65	1.32	1.62	εCH_2: 2.76	−2.78
					1.51		
C-OH	no						

no, not observed; nr, not resolved.

Table 4 The Chemical Shifts (ppm) and Temperature Coefficients of NH Protons of NC(1–11)-OH in DMSO-d_6 at 30 °C

Residue	Chemical shifts (ppm)						$\Delta\delta/\Delta T \times 10^{-3}$
	H_N	α	β	γ	δ	Other	
Phe[1]	no	4.08	3.1			2,6H: 7.32; 3,5H: 7.28	—
			2.94			4: nr	
Gly[2]	8.74	3.79					−4.31
Gly[3]	8.10	3.72					—
		3.67					
Phe[4]	8.13	4.65	3.07			3,5H: 7.28	−4.1
			2.80			2,4,6: nr	
Thr[5]	8.05	4.19	4.01	1.04		OH: 4.82	−4.29
Gly[6]	7.98	3.74					—
Ala[7]	8.00	4.29	1.20				−3.92
Arg[8]	8.05	4.25	1.70	1.48	3.08	εNH_2: 7.53	−4.29
Lys[9]	7.89	4.29	1.67	1.31	1.51	εCH_2 – 2.74; εNH_2 – 7.67	−3.06
Ser[10]	7.94	4.30	3.59				−5.21
Ala[11]	8.07	4.22	1.26				−3.76
C-OH	no						

no, not observed; nr, not resolved.

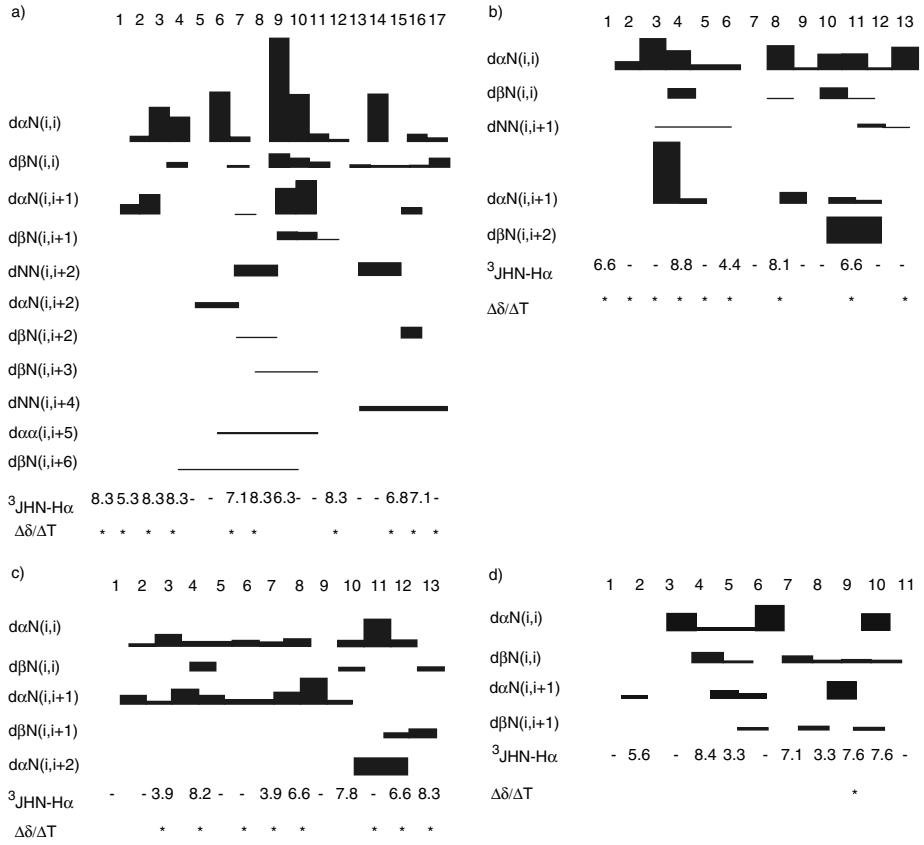

* - lower then -3.5 ppb/K, indicating that the amide proton can be involved in the hydrogen bond or its shielding from solvent

Figure 2 Integral intensities of NOE effects and values of the $^3J_{NH\text{-}H\alpha}$ coupling constants of: (a) NC-NH_2; (b) NC(1–13)-NH_2; (c) NC(1–13)-OH; (d) NC(1–11)-OH obtained in DMSO-d_6.

peptide studied in the second approach is characterized by a set of conformations and their statistical weights. Such calculations were performed with three different force fields. As seen in Table 5, 4–9 conformations were selected with statistical weights higher than 5%. For all the peptides the broad range of values (not shown) did not allow the identification of any predominant conformation(s). The superposition of selected conformations, as well as the ten lowest-energy conformations obtained by distance geometry and SA protocols are shown in Figures 3–6.

The conformations with statistical weights exceeding 5% obtained with the AMBER force field for all peptides studied are shown in Figure 3. The middle fragments of most conformations selected for NC-NH_2 adopt a helical structure. In the case of the conformation with the highest statistical weight (22.6%) only a short fragment, Arg^8-Ala^{11}, displays this element of the secondary structure. But the most possible is the conformation with the second highest statistical weight (21.4%). In this conformation, fragment 4–10 adopts a helical structure. In addition, all four side chains are directed to the outside of the molecule. Side chains of Arg^8 and Arg^{12} are situated on the opposite side of the molecule relative to Lys^9 and Lys^{13}. A similar geometry of the

Table 5 The Number of Low-energy Conformations with Statistical Weights Greater than 5% Obtained in each of the Methods

Peptide	ECEPP/3	AMBER	CHARMM
NC-NH_2	7	6	6
NC(1–13)-NH_2	4	7	4
NC(1–13)-OH	8	9	6
NC(1–11)-OH	7	4	6

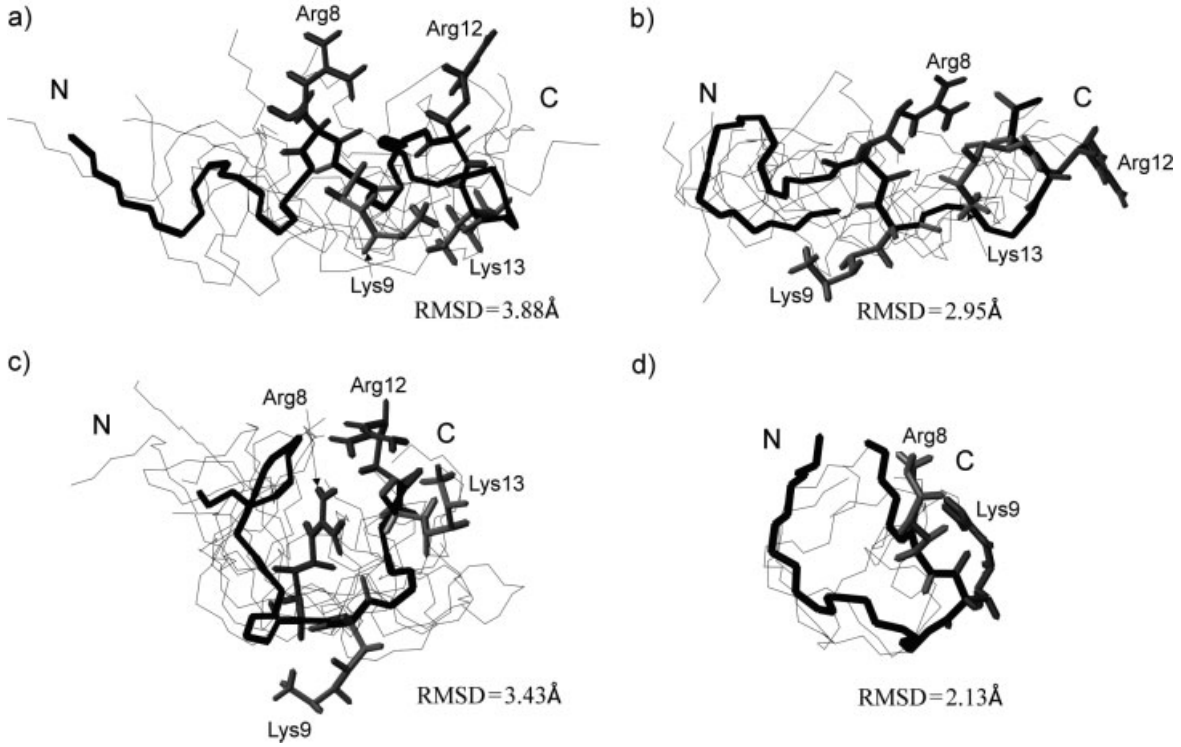

Figure 3 Superposition of low-energy conformations (α-carbon atoms superimposed) with statistical weights higher than 5% of: (a) NC-NH_2; (b) NC(1–13)-NH_2; (c) NC(1–13)-OH; (d) NC(1–11)-OH obtained in the AMBER force field. Bold lines represent backbones and side chains of basic amino acid residues of the conformations with the highest statistical weights.

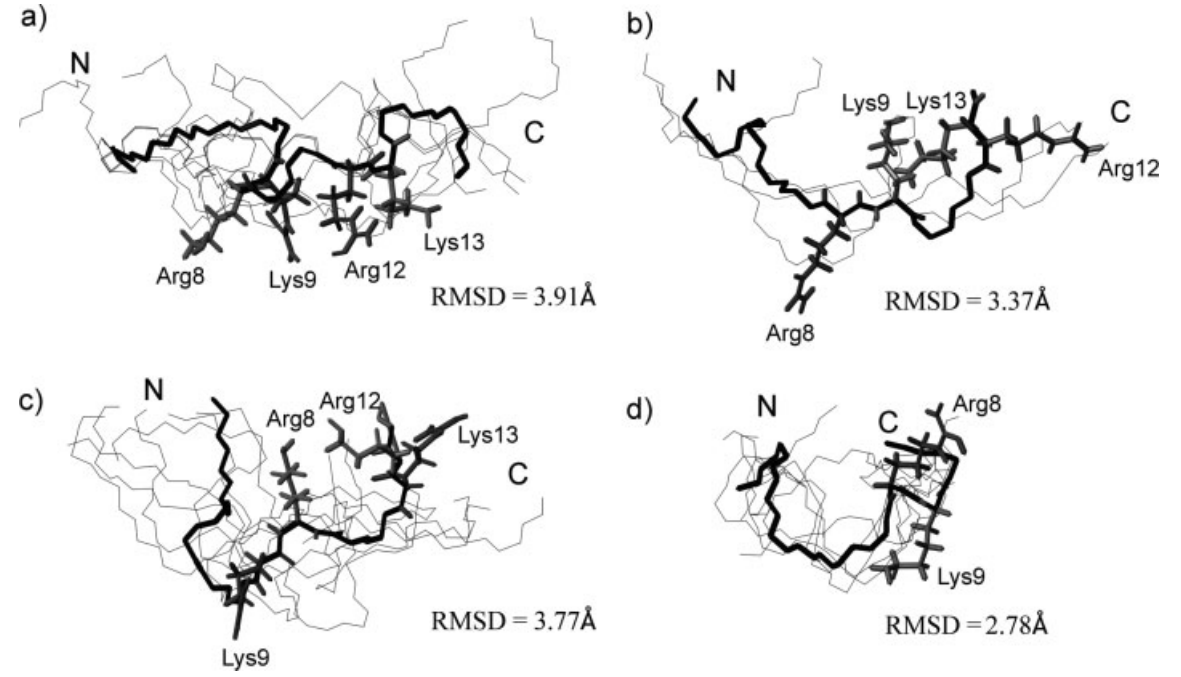

Figure 4 Superposition of low-energy conformations (α-carbon atoms superimposed) with statistical weights higher than 5% of: (a) NC-NH_2; (b) NC(1–13)-NH_2; (c) NC(1–13)-OH; (d) NC(1–11)-OH obtained in the ECEPP/3 force field. Bold lines represent backbones and side chains of basic amino acid residues of the conformations with the highest statistical weights.

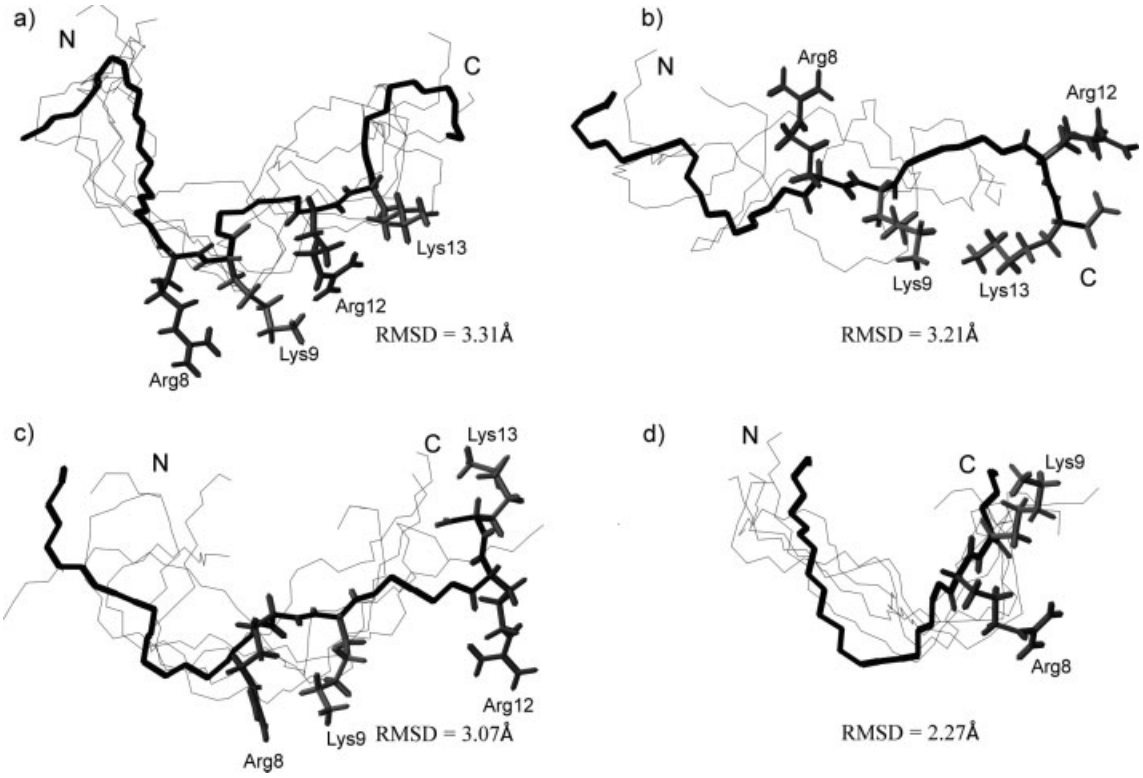

Figure 5 Superposition of low-energy conformations (α-carbon atoms superimposed) with statistical weights higher than 5% of: (a) NC-NH_2; (b) NC(1–13)-NH_2; (c) NC(1–13)-OH; (d) NC(1–11)-OH obtained in the CHARMM force field. Bold lines represent backbones and side chains of basic amino acid residues of the conformations with the highest statistical weights.

peptide backbones was obtained for the conformations of NC(1–13)-NH_2. Also in this case the middle fragments display a helical character. Of the seven conformations selected, two include a helical structure in fragment 4–9 and the other two in fragment 10–12. For the dominant conformation with a statistical weight of 31.4% such a secondary structure element was found in fragment 4–9. Also the side chains of basic amino acid residues are directed to the outside of the molecule. All conformations are stabilized by several hydrogen bonds. The presence of most of them is supported by the calculated values of $\Delta\delta/\Delta T$. Interestingly, the conformations obtained for inactive peptides (NC(1–13)-OH and NC(1–11)-OH) are distinctly different. Their backbones are bent in the middle segments resembling the letter 'υ', some of the basic side chains (e.g. Arg^8 and Arg^{12} for NC(1–13)-OH) are oriented to the inside of the molecule.

All the conformations with statistical weights higher than 5% generated with the ECEPP/3 are shown in Figure 4. Most of the NC-NH_2 conformations display a similar geometry of fragment Arg^8-Ala^{13} (RMSD = 1.54 Å), resembling a helical structure. In the case of the fully active NC(1–13)-NH_2 the backbones of selected conformations adopt an extended structure. In all conformations of these active peptides, the side chains of the basic amino acid residues are exposed outside the molecule. Similar to the results obtained in the AMBER force field, the backbones of the conformations obtained for the less active NC(1–13)-OH and inactive NC(1–11)-OH resemble the letter 'υ'.

All conformations selected for the peptides by the use of the CHARMM force field and calculated by two different approaches are shown in Figures 5 and 6. None of the conformations selected display a helical structure. Nevertheless, the backbones of most conformations of NC-NH_2 obtained by both methods and of NC(1–13)-NH_2 calculated in the CHARMM force field display a similar fold in the Ala^7-Ser^{10} fragment. It allows the side chains of basic amino acid residues to be exposed outside the molecule. The backbones of the conformations obtained for the remaining peptides are bent in the middle fragment, resembling the letter 'υ'.

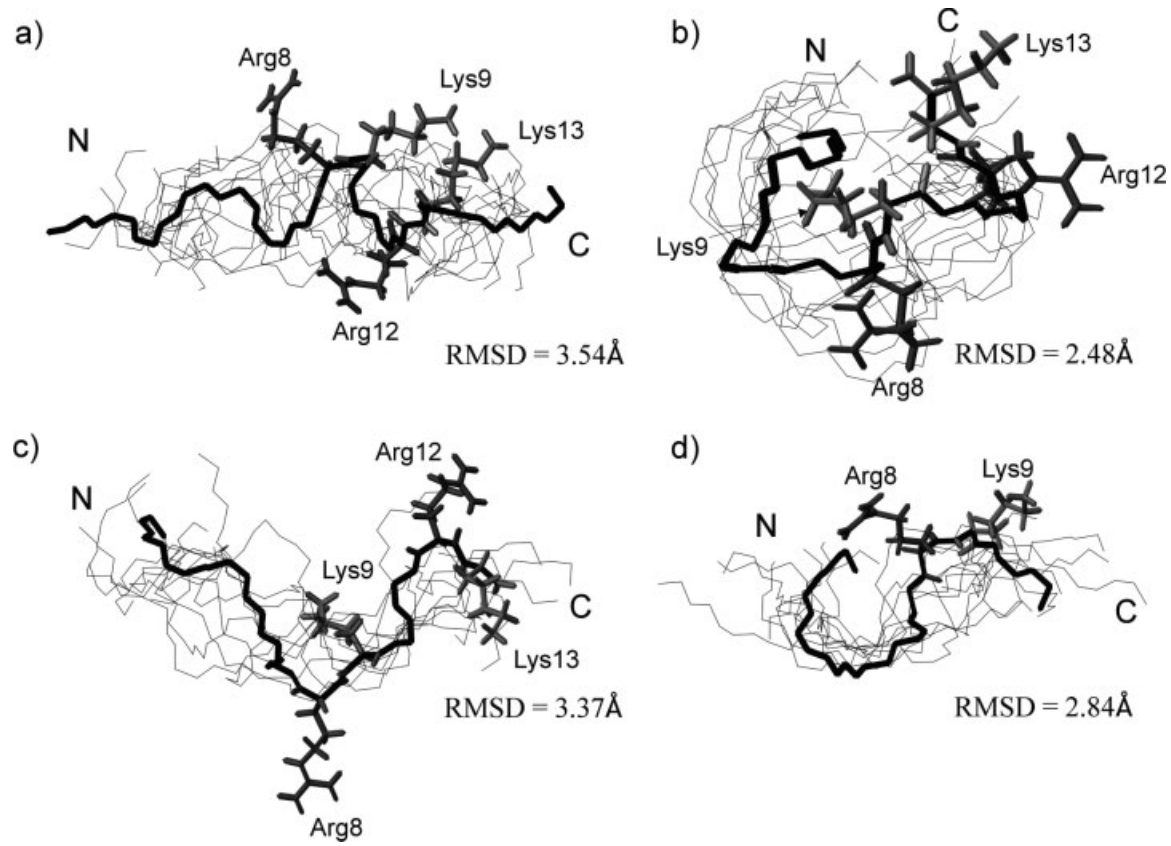

Figure 6 Superposition of 10 lowest-energy conformations (α-carbon atoms superimposed) of: (a) NC-NH_2; (b) NC(1–13)-NH_2; (c) NC(1–13)-OH; (d) NC(1–11)-OH obtained in distance geometry. Bold lines represent backbones and side chains of basic amino acid residues of the lowest energy conformations.

CONCLUSIONS

According to previous reports, fragment 8–13 [7], positions 5 and 6 [37, 38, 39], the β-turn centred on Gly^6-Ala^7 [6] and the basic core [8] are responsible for the receptor's preferences of NC. Very recently, based on the secondary structure prediction and structure–activity relationship studies, Zhang *et al.* [40] have postulated that NC might adopt an amphipathic helix in the address segment (fragment 5–17) of the sequence. Our results discussed above fully support this hypothesis. They indicate the ability of the 8–13 fragment of active NC peptides to form a helical (or helical-like) structure. This might allow for the interaction of the NC peptides (also through the side chains of basic amino acid residues) with the ORL1 receptor. To our knowledge, it is the first time that experimental data indicating a helical character of the NC peptides has been reported. This hypothesis is also supported by the CD investigations. In TFE solutions both ORL1 agonists display a significantly higher content of ordered (probably helical) structure than the remaining two peptides studied. The DMSO- solvent used for the NMR investigations is more polar and therefore its impact on the secondary structure formation is significantly less pronounced, resulting in a high degree of conformational flexibility of the peptides. It is worth noticing that in hydrophobic solvents, dynorphin A, an opioid peptide with high sequential homology to NC, displayed a less ordered structure than in the mixture DMSO/H_2O [5]. In the case of the NC peptides, our CD experiments suggest that for active NC peptides the hydrophobic solvent induced an ordered structure. Thus it is reasonable to assume that the comparison of solution structures of active and inactive NC peptides determined by NMR in a more hydrophobic solvent may allow the structural elements of the NC peptides responsible for their interaction with the ORL1 receptor to be identified.

Acknowledgements

The calculations were carried out in the Academic Computer Center (TASK) in Gdańsk, Poland, and Interdisciplinary Center for Mathematical Modelling (ICM) in Warsaw, Poland. This work was supported by the University of Gdańsk (Grants No. BW-8000-5-0182-1, DS/8290-4-0129-3), grants from the Polish Committee for Scientific Research (KBN No. 3P04B02024) and by the Adam Krzyżanowski Foundation.

REFERENCES

1. Reinscheid RK, Nothecher HP, Bourson A, Ardoti A, Henningen RA, Bunzow JR, Grandy DK, Langen H, Mousma F, Civelli O. Orphanin FQ: a neuropeptide that activates an opioid like G protein-coupled receptor. *Science* 1995; **270**: 792–794.
2. Meunier JC, Mollereau C, Toll L, Snaudeau C, Morisand C, Alvinerie P, Butour JC, Guillemat JC, Ferrara P, Monsarrat B, Mozargull H, Vassart G, Parmetier M, Constentin J. Isolation and structure of the endogenous agonist of opioid receptor-like ORL1 receptor. *Nature* 1995; **377**: 532–535.
3. Suder P, Kotlińska J, Smoluch M, Silberring J, Sallberg M. Metabolic fate of nociceptin/orphanin FQ in the rat spinal cord and biological activity of its released fragment. *Peptides* 1999; **20**: 239–247.
4. Salvadori S, Picone D, Tancredi T, Guerrini R, Spadaccini R, Lazarus LH, Regoli D, Temussi PA. Solution conformation of nociceptin. *Biochem. Biophys. Res. Commun.* 1997; **233**: 640–643.
5. Spadaccini R, Crescenzi O, Picone D, Tancredi T, Temussi PA. Solution structure of dynorphin A (1–17): a NMR study in a cryoprotective solvent mixture at 278K. *J. Peptide Sci.* 1999; **5**: 306–312.
6. Amodeo P, Guerrini R, Picone D, Salvadori S, Spadaccini R, Tancredi T, Temussi PA. Solution structure of nociceptin peptides. *J. Peptide Sci.* 2002; **8**: 497–509.
7. Guerrini R, Calo G, Rizzi A, Bianchi C, Lazarus L, Salvadori S, Temussi PA, Regoli D. Address and message sequences for the nociceptin receptor: a structure-activity study of nociceptin-(1–13)-peptide amide. *J. Med. Chem.* 1997; **40**: 1789–1793.
8. Salvadori S, Guerrini R, Calo G, Regoli D. Structure-activity studies on nociceptin/orphanin FQ: from full agonist, to partial agonist, to pure antagonist. *Il Farmaco* 1999; **54**: 810–825.
9. Suder P, Kotlińska J, Łęgowska A, Smoluch M, Höhne G, Chervet J-P, Rolka K. Silberring J. Determination of nociceptin-orphanin FQ metabolites by capillary LC-MS. *Brain Res. Prot.* 2000; **6**: 40–46.
10. Bax A, Davis DG. MLEV-17 based two-dimensional homonuclear magnetization transfer spectroscopy. *J. Magn. Reson.* 1985; **65**: 355–360.
11. Piantini U, Sørensen OW, Ernst RR. Multiple quantum filter for elucidating NMR coupling networks. *J. Am. Chem. Soc.* 1982; **104**: 6800–6801.
12. Rance M, Sørensen OW, Bodenhausen G, Wagner G, Ernst RR, Wüthrich K. Improved spectral resolution in COSY ^{1}H NMR spectra of proteins via double quantum filtering. *Biochem. Biophys. Res. Commun.* 1983; **117**: 479–485.
13. Jeener J, Meier BH, Bachmann P, Ernst RR. Investigation of exchange process by two-dimensional NMR spectroscopy. *J. Chem. Phys.* 1979; **71**: 4546–4563.
14. Bodenhausen G, Kogler H, Ernst RR. Selection of coherence-transfer pathways in pulse NMR experiments. *J. Magn. Reson.* 1984; **58**: 370–388.
15. Bothner-By AA, Stephens RL, Lee J-M, Warren CD, Jeanloz RW. Structure determination of a tetrasaccharide: Transient nuclear Overhauser effects in the rotating frame. *J. Am. Chem. Soc.* 1984; **106**: 811–813.
16. Bax A, Davis DG. Practical aspects of two-dimensional transverse NOE spectroscopy. *J. Magn. Reson.* 1985; **63**: 207–213.
17. Bartels CT, Billeter M, Güntert P, Wüthrich K. The program XEASY for the computer-supported NMR spectral analysis of biological macromolecules. *J. Biomol. NMR* 1995; **6**: 1–10.
18. MestRe-C Version 2.3 — Magnetic Resonance Companion. Departamento de Quimica Organica, Facultad de Quimica, Universidad de Santiago de Compostela, Santiago de Compostela, Spain; http://qobrue.usc.es/jsgroup/MestRe-C/MestRe-C.html.
19. Güntert P, Wüthrich K. Efficient computation of three dimensional protein structures in solution form nuclear magnetic resonance data using the program DIANA and the supporting programs CALIBA, HABAS and GLOMSA. *J. Mol. Biol.* 1991; **217**: 517–530.
20. Ripoll DR, Scheraga HA. On the multiple-minima problem in the conformational analysis of polypeptides, II. An electronically driven Monte Carlo method — tests on poly(L-alanine). *Biopolymers* 1988; **27**: 1283–1303.
21. Némethy G, Gibson KD, Palmer KA, Yoon CN, Paterlini G, Zagari A, Rumsey S, Scheraga HA. Energy parameters in polypeptides. 10. Improved geometrical parameters and nonbonded interactions for use in the ECEPP/3 algorithm with application to proline-containing peptides. *J. Phys. Chem.* 1992; **96**: 6472–6484.
22. Groth M, Malicka J, Rodziewicz- Motowidlo S, Czaplewski C, Klaudel L, Wiczk W, Liwo A. Determination of conformational equilibrium of peptides in solution by NMR spectroscopy and theoretical conformational analysis: application to the calibration of mean-field solvation models. *Biopolymers* 2001; **60**: 79–95.

23. Pearlman DA, Case JW, Caldwell JW, Ross WS, Cheatham TE, Ferguson D, Seibel GL, Singh UC, Weiner P, Ollman PA. *AMBER 4.1, 1995*. University of California, San Francisco.
24. Case DA, Pearlman DA, Caldwell JW, Cheatham III TE, Ross WS, Simmerling CL, Darden TA, Merz KM, Stanton RV, Cheng AL, Vincent JJ, Crowley M, Ferguson DM, Radmer RJ, Seibel GL, Singh UC, Weiner PK, Kollman PA. *AMBER 5, 1997*. University of California, San Francisco.
25. Brooks B, Bruccoleri R, Olafson BO, States DJ, Swaminathan S, Karplus M. CHARMM a program for macromolecular energy minimization and dynamics calculations. *Comp.Chem.* 1983; **4**: 187–217.
26. Brünger AT. *The X-PLOR Software Manual, Version 3.1, 1992*. Yale University Press: New Haven, CT.
27. Ripoll DR, Pottle MS, Gibson KD, Liwo A, Scheraga HA. Implementation of the ECEPP algorithm, the Monte Carlo minimization method. *J. Comput. Chem.* 1995; **16**: 1153–1163.
28. Späth H. Cluster analysis algorithms. *J. Comput. Chem.* 1980; **10**: 209–220.
29. Groth M, Malicka J, Czaplewski C, Liwo A, Łankiewicz L, Wiczk W. Maximum entropy approach to the determination of solution conformation of flexible polypeptides by global conformational analysis and NMR spectroscopy — application to DNS^1-c[D-A_2bu^2, Trp^4, Leu^5]-enkephalin and DNS^1-c[D-A_2bu^2, Trp^4,D-Leu^5]-enkephalin. *J. Biomol. NMR* 1999; **15**: 315–330; http://www.tc.cornell.edu/resource/CompBiologyTools/analyze.
30. Massefski WJ, Bolton PH. Quantitative analysis of nuclear Overhauser effects. *J. Magn. Reson.* 1985; **65**: 526–530.
31. Meadows RP, Post CB, Luxon BA, Gorenstein DG. *MORASS 2.1, 1994*. Purdue University, W. Lafayette.
32. Post CB, Meadows RP, Gorenstein DG. On the evaluation of interproton distance for 3-dimentional structure determination by NMR using a relaxation rate matrix analysis. *J. Am. Chem. Soc.* 1990; **112**: 6796–6803.
33. Bystrov VF. Spin-spin coupling and the conformational states of peptide system. *Progr. NMR Spectrosc.* 1976; **10**: 41–81.
34. Powell MJD. Restart procedures for conjugate grdient method program. *Math. Prog.* 1977; **12**: 241–254.
35. Crisma M, Fasman GD, Balaram H, Balaram P. Peptide models for beta-turns. A circular dichroism study. *Int. J. Pept. Protein Res.* 1984; **23**: 411–419.
36. Hollosi M, Kawai M, Fasman GD. Studies on proline-containing tetrapeptide models of beta-turns. *Biopolymers* 1985; **24**: 211–242.
37. Topham CM, Mouledous L, Poda G, Maigret B, Meunier JC. Molecular modelling of the ORL1 receptor and its complex with nociceptin. *Protein Eng.* 1998; **11**: 1163–1179.
38. Lapalu S, Moisand C, Mazarguil H, Cambois G, Mollereau C, Meunier JC. Comparison of the structure-activity relationship of nociceptin and dynorphin A using chimeric peptides. *FEBS Lett.* 1997; **417**: 333–336.
39. Okada K, Sujaku T, Chuman Y, Nakashima R, Nose T, Costa T, Yamada Y, Yokoyama M, Nagahisa A, Shimohigashi Y. Highly potent nociceptin analogue containing the Arg-Lys triple repeat. *Biochem. Biophys. Res. Commun.* 2000; **278**: 493–498.
40. Zhang C, Miller W, Valenzano KJ, Kyle DJ. Novel potent ORL-1 receptor agonist peptides containing α-helix promoting conformational constraints. *J. Med. Chem.* 2002; **45**: 5280–5286.

